JOURNAL OF CATALYSIS 152, 264–274 (1995)

CO Adsorption and Oxidation on Pt(111) Electrodes Modified by Irreversibly Adsorbed Bismuth in Sulfuric Acid Medium

E. Herrero, J. M. Feliu, and A. Aldaz

Departament de Química-Física, Universitat d'Alacant, Ap. Correus 99, E-03080 Alacant, Spain

Received January 31, 1994; revised October 31, 1994

CO adsorption and desorption ("stripping") on Pt(111) electrodes modified by irreversibly adsorbed bismuth have been studied. The presence of CO adsorbed on the Bi–Pt(111) electrode modifies the redox peak of the adsorbed bismuth, suggesting the presence of a CO–Bi mixed adlayer. Using the CO stripping charge after appropriate correction, the values of CO coverage for the different bismuth coverages were calculated, as well as the proportions of linear and bridged-bonded CO. Unlike in UHV environments, the presence of bismuth on the surface favors the linear configuration of the adsorbed CO. At $\Theta_{Bi} = 0.15$, the CO population is almost entirely constituted linear CO, regardless of the CO coverage. Transient CO stripping demonstrates that the presence of bismuth on the surface enhances CO oxidation through bismuth-mediated oxygen transfer. © 1995 Academic Press, Inc.

INTRODUCTION

Carbon monoxide is a small molecule that adsorbs on many different metal surfaces. Because of its simplicity, it can be considered as a test molecule for adsorption. In UHV, this molecule has been widely studied both on unmodified Pt(111) surfaces (1–6) and on adatom-modified Pt(111) surfaces (7, 8). Interest in the behavior of this molecule in electrochemical environments has arisen only recently, when electrode preparation techniques suitable for bare single-crystal electrodes (9) and modified single crystals were developed (10).

On Pt(111) electrodes, the CO molecule can adsorb mainly in two different configurations; namely either in a linear form, in which the CO molecule is bonded through the carbon atom to one platinum atom, or in a bridged-bonded configuration, in which the molecule is bonded to two adjacent platinum atoms (11–16). In addition, multibonded CO has also been detected for saturation CO coverages and electrode potentials near hydrogen evolution (15, 17). *In situ* IR studies have demonstrated that the ratio between the populations of the different configurations depends on the CO coverage and potential (13, 15). For instance, a transformation from multibonded CO to bridge-bonded CO is observed as the electrode potential moves from 0.1 to 0.4 V (15).

On the other hand, Pt(111) electrodes can be easily modified by bismuth, using the irreversible adsorption dosing technique (10). This method provides bismuth-modified electrodes with different bismuth surface concentrations, whose bismuth coverage can be calculated using electrochemical methods. The maximum stable coverage attainable with this technique is 0.33 (10), but higher coverages can be achieved (18, 19). Using these modified electrodes, the oxidation of formic acid (20) and methanol (21) and poison formation from formic acid and methanol (22) have been studied.

To our knowledge, only one study has previously been made of CO adsorption on bismuth-modified Pt(111) electrodes in perchloric acid medium (23). In this work, in which CO adsorption was studied using *in situ* Fourier transform infrared (FTIR) spectroscopy, it was found that at the highest bismuth coverage studied (0.21), CO is adsorbed almost exclusively as linearly bonded CO, irrespective of the CO coverage. Based on variations in CO absorbance and in the relative populations of linear and bridged-bonded CO with the bismuth coverage, a microscopically mixed structure for the CO–Bi adlayer was proposed.

In the present work, CO adsorption and oxidation have been studied on Pt(111) electrodes with bismuth coverages ranging between 0 and 0.33, using purely electrochemical methods. The variations in the voltammetric profile of the modified electrode allow the influence of CO in the bismuth adlayer to be determined and a possible structure for the CO–Bi adlayer to be proposed. The CO stripping charge after appropriate corrections (24) serves to calculate CO coverages and the relative populations of the CO configurations. In this correction, the bismuth oxidation charge and the charge of the unusual states (the voltammetric features that appear between 0.3 and 0.5 on unmodified Pt(111) electrodes (25)) have been subtracted from the uncorrected CO oxidation charge. Comparison with the IR results (23) has been useful to verify the

0021-9517/95 $6.00

electrochemical method of CO coverage calculation. Finally, the influence of surface bismuth on the CO oxidation kinetics has also been studied.

METHODS

Pt(111) electrodes have been oriented within ±3′, cut and polished down to 0.25 μm with diamond paste from small single crystal beads according to the technique of Clavilier *et al.* (26). All coverages have been defined as the number of adsorbed species per platinum atom. All potentials have been measured versus the reversible hydrogen electrode (RHE).

The experimental protocol is as follows:

(i) Irreversible adsorption of bismuth is carried out spontaneously by immersion of the clean Pt(111) electrode in a Bi(III)-containing solution, as has been described elsewhere (10). This modified electrode is characterized in the test electrolyte (0.5 *M* sulfuric acid solution free of Bi(III) species) in a potential range that assures the stability of the electrode substrate structure as well as the bismuth adsorbed on the surface (0.06–0.85 V). The bismuth coverage is calculated from the charge of the surface redox process of the adsorbed bismuth, assuming that bismuth exchanges two electrons, or from the platinum adsorption charge (10) using the equations

$$\Theta_{Bi} = \frac{\frac{1}{2}Q_{Bi}}{241} \quad [1]$$

$$\Theta_{Bi} = \tfrac{1}{3}\left(1 - \frac{Q_{Pt}^{Bi}}{241}\right), \quad [2]$$

where Q_{Bi} is the bismuth oxidation charge (Fig. 1B, light shadowed area), Q_{Pt}^{Bi} the platinum adsorption charge of the electrode covered by bismuth (Fig. 1B, dark shadowed area), and 241 $\mu C\ cm^{-2}$ the platinum adsorption charge of the unmodified Pt(111) electrode for a monoelectronic surface adsorption process involving all surface platinum atoms (1.5×10^{15} atoms cm^{-2}). Both equations give the same coverage within experimental error. The maximum stable bismuth coverage attainable with this method in the potential range studied is 0.33, implying that bismuth blocks three platinum adsorption sites. This value coincides with the mean value obtained by Shibata and coworkers for polycrystalline electrodes (27).

(ii) Afterwards, CO adsorption is carried out from a CO saturated solution in 0.5 *M* sulfuric acid at open circuit as described in Ref. (28). Depending on the desired CO coverage, the adsorption time ranges from 2 s to 2 min. After CO adsorption, the electrode is immersed in the test electrolyte and the CO contained in the droplet attached to the electrode is dispersed by argon bubbling.

(iii) The voltammetric profile between 0.05 and 0.5 V is recorded to point out the CO blocking and then CO is desorbed (stripped) from the electrode surface, with the upper potential limit at 0.85 V to avoid any electrochemical desorption of the bismuth adlayer. After CO stripping, a new voltammogram is recorded. This allows comparison of the initial and final states of the electrode in the entire experiment.

RESULTS AND DISCUSSION

Evidence of a Bi–CO-Mixed Adlayer on Pt(111)

Figure 1 shows the results of the CO stripping experiment obtained for four different bismuth coverages on a Pt(111) electrode. After CO adsorption, all platinum adsorption sites have been blocked and only capacitive processes of double layer charging–discharging can be detected in the region 0.06–0.50 V, giving a flat voltammetric profile in this region.

On clean Pt(111) surfaces, the onset of CO oxidation is at 0.75 V (excluding small prewaves at around 0.6 V (Fig. 2)). The presence of bismuth has shifted the onset of CO oxidation to a lower potential value (0.6 V). This potential value is also the onset for bismuth surface oxidation on the Pt(111) electrode, but as Fig. 1 shows, the surface redox peak of bismuth does not appear at its usual potential (0.625 V). In contrast, a split peak appears in the region 0.70–0.85 V, which corresponds to the CO oxidation process and other surface processes. After CO oxidation, the reduction peak of the surface bismuth can be observed at its usual potential. Hence, bismuth has been oxidized along with the adsorbed CO, and the oxidation process between 0.60 and 0.85 V has to be attributed to the joint oxidation of bismuth and CO (Fig. 1B). However, the first reduction peak of the surface bismuth is lower than that appearing in the subsequent scans (Fig. 1). This indicates that part of the bismuth adatoms have already been reduced. One possible explanation of this fact is that the oxidized bismuth is providing the oxygen necessary for CO oxidation. When the scan is reversed at 0.85 V, the residual CO is oxidized to CO_2 by the surface Bi(II), and the Bi(II) is reduced to Bi^0, thus diminishing the amount of Bi(II) that can be reduced at 0.625 V. This hypothesis will be confirmed later.

As has already been mentioned, the CO oxidation occurs in a split peak. As neither peak involves higher charge than the bismuth oxidation charge, neither can be strictly assigned to this process, and the splitting must be attributed to kinetic complications induced by the presence of bismuth on the surface, as will be discussed later. Occasional CO oxidation prewaves may occur, as found for unmodified Pt(111) electrodes (24) (Fig. 2).

It is remarkable that the presence of small amounts of bismuth already exerts an influence on the CO stripping

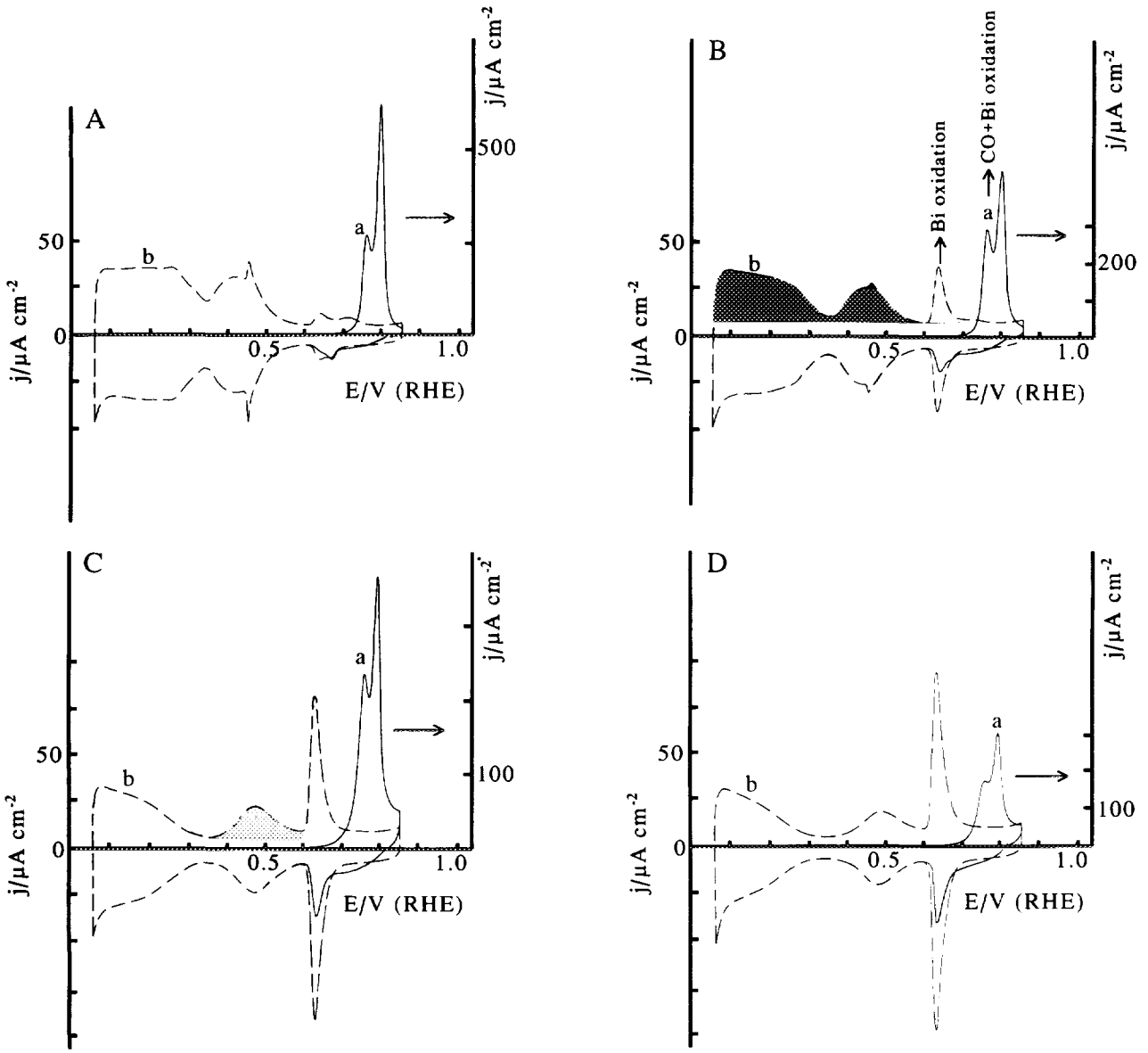

FIG. 1. CO stripping experiment for a Pt(111) electrode with different bismuth coverages at maximum CO coverage. (A) $\Theta_{Bi} = 0.01$, (B) $\Theta_{Bi} = 0.10$, (C) $\Theta_{Bi} = 0.14$, and (D) $\Theta_{Bi} = 0.20$. (a) Stripping of the adsorbed CO, (b) recovery of the adsorptive properties of the electrode after the CO stripping (dashed line). Scan rate 50 mV s^{-1} in all voltammograms. For explanation of shadowed areas, see text.

process. Voltammetric CO oxidation on clean Pt(111) (Fig. 2) occurs in a sharp peak around 0.83 V. In contrast, the presence of bismuth at $\Theta_{Bi} = 0.01$ (Fig. 1A) gives a broader and split peak at potentials around 0.75 and 0.80 V. This differs from the earlier observations of Chang and Weaver (23), where no significant differences in CO oxidation induced by the presence of bismuth were reported. In this latter work, $HClO_4$ medium was used as supporting electrolyte. In $HClO_4$, CO oxidation occurs at more negative potentials and the shift of the CO oxidation has masked the effect of bismuth on CO oxidation.

Coadsorbed CO and bismuth can present two different surface structures; either with segregated domains, where CO and bismuth are adsorbed on different islands with higher local coverage than the corresponding overall coverage, or in a microscopically mixed adlattice. The potential shift of the onset of the CO stripping suggests the second explanation to be the more suitable. The influence of CO adsorption on the bismuth redox peak allows one to gain insight into this issue. As has been pointed out (10), the oxidation of the surface bismuth involves the presence of an oxygenated species, probably $Bi(OH)_2$ or

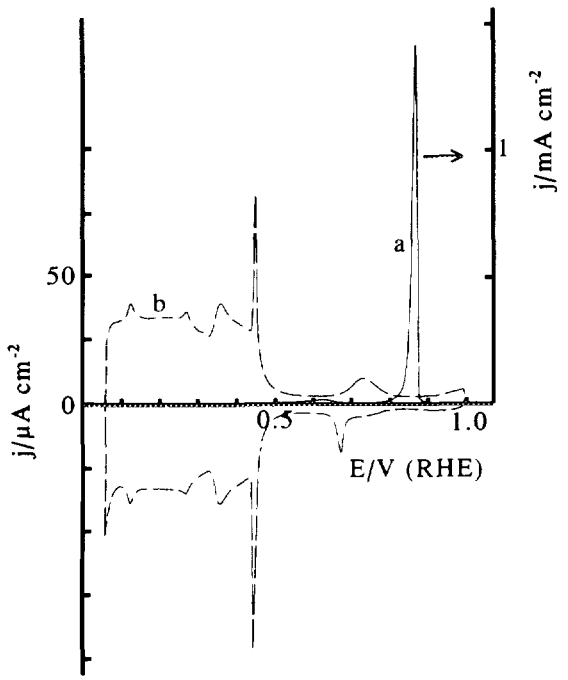

FIG. 2. CO stripping experiment for an unmodified Pt(111) electrode at maximum CO coverage. (a) and (b) as in Fig. 1.

BiO. In 0.5 *M* H_2SO_4, water must supply the oxygen involved in the oxidation of the bismuth at 0.625 V. If the CO–Bi adlattice were constituted by segregated domains, the local coverage of the bismuth islands would be higher than the mean value and the influence of the CO in the bismuth adlayer would be limited to the border between the segregated domains. This being so, the presence of CO on the surface would only affect the bismuth adatoms near the border of the island. The rest of the bismuth island, where no influence of the CO adatoms is expected, would have an oxidation mechanism similar to that observed at the local bismuth coverage inside the island. This local coverage would be probably near 0.33, which is the maximum stable coverage of bismuth on Pt(111) electrodes. At $\Theta_{Bi} = 0.33$, all platinum adsorption sites have been blocked by the adatoms, but the redox peak appears at its usual value (0.625 V) (10). As the redox peak does not appear at its usual potential values, CO is affecting the electrochemical behavior of all bismuth adatoms and a mixed adlayer is proposed as the most probable structure of the Bi–CO adlayer.

Partial desorption of CO also supports the idea of a mixed adlayer. If the scan is reversed at the beginning of CO oxidation, the bismuth reduction peak can be seen in the subsequent positive-going scan along with part of the platinum adsorption sites which have been restored. At medium and high bismuth coverages, partial desorption of CO only partially restores the bismuth oxidation–reduction peak which appears at its usual peak potential of 0.625 V (Fig. 3). This suggests that the surface bismuth oxidation at the usual potential value only occurs in the zones where CO oxidation has taken place. Also, the beginning of CO oxidation has to occur through points where CO and bismuth are in contact. Once the CO is stripped in the surroundings of the bismuth adatom, some free adsorption platinum sites are created. Only those bismuth adatoms without lateral interactions with CO adsorbed molecules can be oxidized at the usual potential values. Therefore, the presence of lateral interactions modifies the potential for the bismuth and CO oxidation processes. The presence of bismuth can also have an influence on the amount of adsorbed CO, but in any case the CO stripping charge at upper potential limit should involve all the adsorbed CO molecules.

Some modifications of the electrode properties occur after CO oxidation (Fig. 4). The recovery factor, S_r, (ratio between the charge of the platinum adsorption states after and before CO adsorption and oxidation) is always greater than 1, as a result of partial desorption of bismuth. The bismuth desorption is generally small, and it is only significant when the initial bismuth coverage is greater than

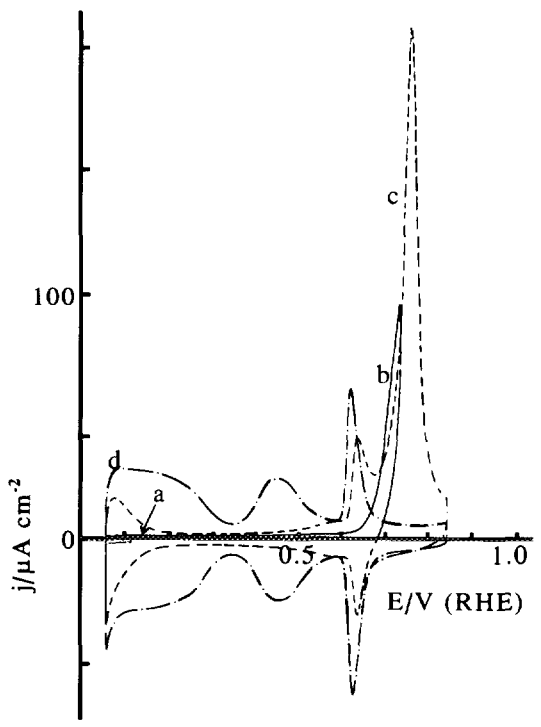

FIG. 3. Partial desorption of CO experiment for a Pt(111) electrode with $\Theta_{Bi} = 0.14$ at maximum CO coverage. (a) Initial electrode state after CO adsorption, (b) partial CO stripping, (c) voltammogram of the electrode after the partial stripping and stripping of the remaining CO (dashed line), and (d) voltammogram of the electrode after total CO stripping (dashed-dotted line).

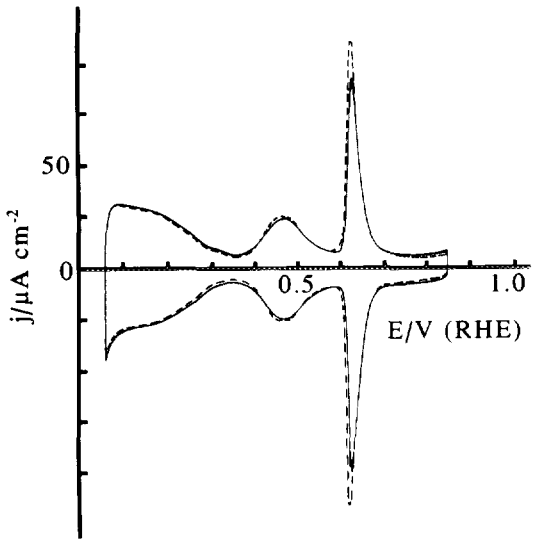

FIG. 4. Voltammogram of a Pt(111) electrode with $\Theta_{Bi} = 0.11$ before CO adsorption (dashed line) and after CO stripping (full line).

0.20. Hence, adsorption of CO is competitive with adsorption of bismuth. The presence of a mixed adlayer Bi–CO on Pt(111), which probably has an ordered structure, may require that some bismuth adatoms be desorbed to reach a more stable structure. This should occur especially at high bismuth coverages where the surface is almost completely blocked by bismuth.

When the electrode was initially prepared, the relationship between the charge of the platinum adsorption states and the bismuth redox charge (10),

$$Q_{Pt}^{Bi} + \tfrac{3}{2}Q_{Bi} = 241\ \mu C\ cm^{-2}, \qquad [3]$$

is always fulfilled. After CO oxidation there is always less Q_{Bi} charge than that corresponding to this Q_{Pt}^{Bi}, as a result of a diminution of the charge beneath the bismuth redox peak. Parallel to this diminution, there is a broadening of the region between 0.7 and 0.85 V in the voltammogram. This behavior can be due to the formation of an alloy, resulting in the modification of the initial properties of the electrode. In any case, the alloy formation is restricted to small regions, since the difference of $Q_{Pt}^{Bi} + 3/2\ Q_{Bi}$ with respect to the beginning of the experiment is always lower than 10%, although occasionally higher differences may be found.

Additional evidence of the presence of mixed adlayers is found studying nonsaturation CO coverages. For the sake of comparison, two different bismuth coverages have been chosen and different CO coverages have been obtained by changing the CO dosing time. As the CO adsorption induces the small changes in the modified electrode stated above, irreversible adsorption of bismuth on a fresh, flame-annealed electrode was always carried out prior to every experiment. The bismuth coverages chosen were $\Theta_{Bi} = 0.05 \pm 0.01$ and $\Theta_{Bi} = 0.15 \pm 0.01$. Coverages higher than 0.20 are not suitable for these experiments since bismuth desorption at high CO coverages is more important.

Figure 5 shows the voltammetric profiles corresponding to two different CO coverages for $\Theta_{Bi} = 0.05$. At low CO coverages (Fig. 5A), the bismuth redox peak appears at its usual potential. Therefore, no lateral interactions are detected between CO and the bismuth adlayer. At these stages mixed adlayers should not be formed. As observed with unmodified Pt(111) surfaces (28), the CO stripping process is shifted to lower potential values as compared to the saturation coverage (fully blocked surface).

If the CO electrode surface becomes more blocked by adsorbed CO (Fig. 5B), the bismuth redox peak begins to shift to higher potential values and involves lower charge than in the initial voltammogram. Lateral interactions become important and the CO peak splits. At these CO coverages, the mixed adlayer is probably formed. The shift of the bismuth redox peak toward more positive potential values suggest increasing lateral interaction of the bismuth adatoms with the adsorbed CO, but not so important as to prevent bismuth surface oxidation prior to CO stripping. This implies that part of the bismuth adatoms are not completely surrounded by CO and the mixed adlayer is not entirely formed.

For $\Theta_{Bi} = 0.15$, the behavior is the same (Fig. 6). Only at near-saturation CO coverages can an interaction between the CO and bismuth adsorbed on the surface be detected.

The presence of mixed adlattices has also been proposed in *in situ* FTIR (23) studies. In this latter case the interaction Bi–CO was proposed after studying the influence of bismuth adatoms on the ν_{CO} distribution as compared to the unmodified Pt(111) surfaces. In our cases the presence of mixed adlayers has been suggested by studying the variation of the bismuth redox peak with the potential. The mixed CO–Bi adlattice has also been suggested for this system in UHV (7), although direct comparison with UHV environments is not always straightforward.

CO Charge Measurements

The most important problem in performing a quantitative analysis of the CO coverage is to determine the correction which has to be applied to the charge measurements of the CO stripping process. In this work, the criterion described in Ref. (24) has been followed and modified to adapt it to the presence of bismuth on the surface.

At the onset of CO oxidation, the electrode has a double

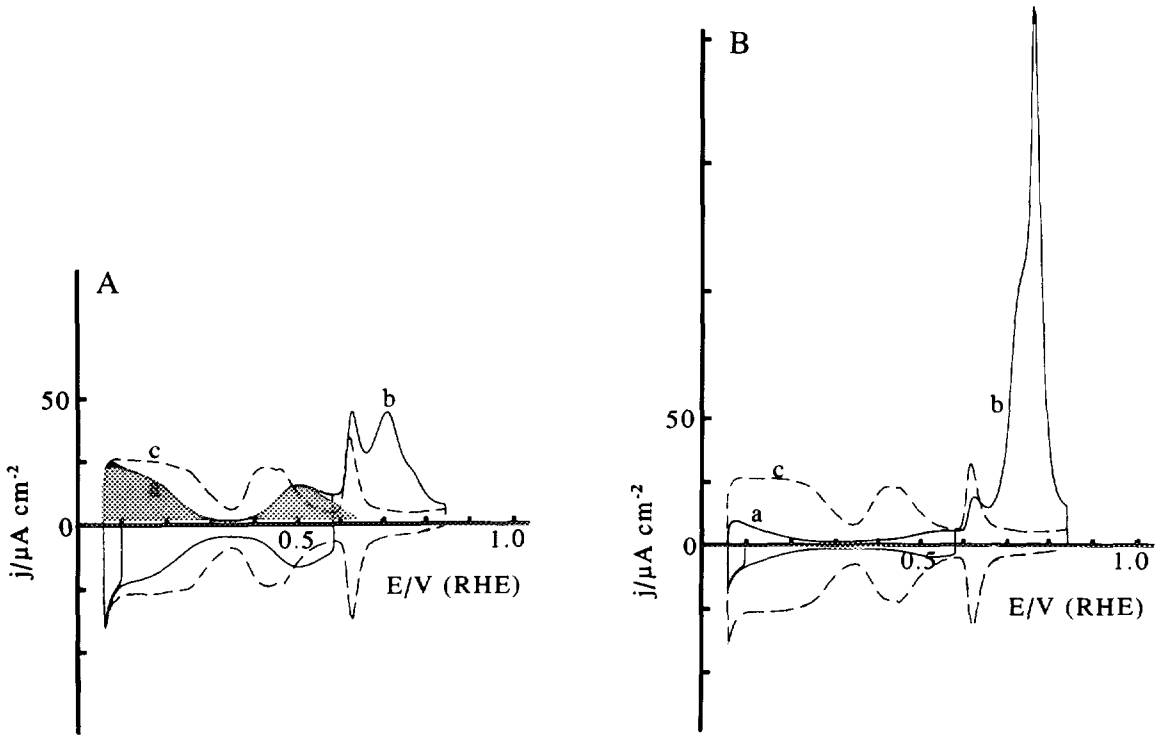

FIG. 5. Two different CO stripping experiments for a Pt(111) electrode with Θ_{Bi} = 0.05 at partial CO coverages. (a) Initial electrode state after CO adsorption, (b) CO stripping, and (c) recovery of the adsorptive properties of the electrode after the CO stripping (dashed line). For explanation of shadowed area, see text.

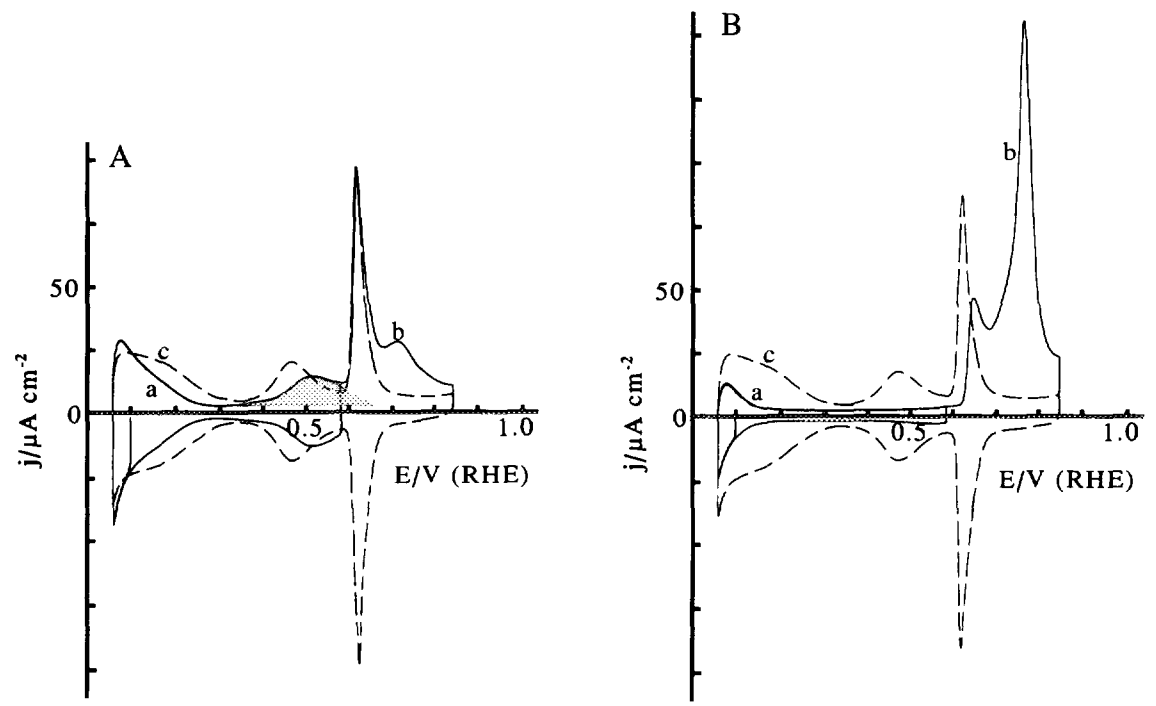

FIG. 6. Two different CO stripping experiments for a Pt(111) electrode with Θ_{Bi} = 0.15 at partial CO coverages. (a), (b), and (c) as in Fig. 5. For explanation of shadowed area, see text.

layer charge and after CO stripping, a charge transfer due to the modification of the double layer capacitances, the oxidation of bismuth adatoms and CO oxidation has occurred. Besides, if anions are responsible for the unusual states, as is concluded from the experiments of CO displacement (29, 30), an additional charge transfer has occurred during CO stripping to restore the adsorption charge of these unusual states. Thus, the overall charge measured in the stripping of CO can be written as

$$q_{CO} = Q_{CO} + (Q_f - Q_i), \quad [4]$$

where q_{CO} is the overall charge measured in the whole CO stripping process (without any double layer correction), Q_{CO} is the charge corresponding to the true CO oxidation process, and Q_f and Q_i are the charges involved in the other surface processes (double layer charge, anion adsorption, . . .), which have occurred at the onset and after CO oxidation, respectively. Q_f can be written as

$$Q_f = (E_f - E^{Bi}_{pzc})K^{Bi} + Q^{unusual}_{Pt} + Q_{Bi}, \quad [5]$$

where $(E_f - E^{Bi}_{pzc})K^{Bi}$ is the capacitive term, E_f is the upper limit potential (0.85 V), E^{Bi}_{pzc} is the point of zero charge (pzc) of the electrode with bismuth, K^{Bi} is the integral capacity of the electrode, $Q^{unusual}_{Pt}$ (Fig. 1C, shadowed area) is the charge of the unusual states, and Q_{Bi} (Fig. 1B, light shadowed area) is the oxidation charge of the bismuth adatoms.

At the onset of CO oxidation the electrode charge has two terms, namely a pure capacitive charge and also the remaining charge of unusual states after CO adsorption

$$Q_i = (E_i - E^{CO}_{pzc})K^{CO} + Q^{unusual,CO}_{Pt}, \quad [6]$$

where E_i is the onset of CO oxidation, E^{CO}_{pzc} is the pzc of the electrode covered by CO, K^{CO} is the capacity of this latter electrode, and $Q^{unusual,CO}_{Pt}$ is the charge of the unusual adsorption states after CO adsorption (Fig. 6A, shadowed area). This term is zero when CO saturation layers are obtained.

The main problem in calculating exactly the values of Q_f and Q_i is to know the pzc of the electrodes. Precise values of the pzc are not even available for the clean Pt(111) electrodes, but an estimate can be made (24). As already mentioned, the unusual states are linked to the presence of adsorbed bisulfate (31, 32). Then, the pzc must be around the potential value where almost all bisulfate species have been desorbed. The only radiometric data available are on 10^{-3} M H_2SO_4 (31), but taking into account the shift in the onset of bisulfate adsorption due to the increase of concentration, the pzc should be approximately at 0.3 V for the unmodified Pt(111) electrode in 0.5 M H_2SO_4. For the bismuth-covered electrode, the unusual states shift slightly to more positive potentials with the bismuth coverage, but as a general criterion the pzc can be maintained at 0.3 V. At $\Theta_{Bi} > 0.15$, the pzc may have shifted to 0.35 V, so the criterion of $E^{Bi}_{pzc} = 0.3$ would underestimate the CO charge. However, as the capacitance of the double layer diminishes with the bismuth coverage, the difference between both corrections lies within the experimental error. For the CO-covered electrode, the pzc is also taken as 0.3 V (24). In any case, these additional corrections related to the pzc shift are much lower than that related to the unusual states.

As the electrode suffers small modifications due to CO adsorption, two Q_f corrections can be calculated: one for the initial state of the electrode and the other after CO stripping. However, as the modifications of the electrode seem to be a consequence of the CO adsorption and not of the CO oxidation, Q_f values are always reported from the voltammogram obtained after CO adsorption and stripping.

Using this correction and assuming that two electrons are transferred in the CO oxidation to CO_2, a value of $\Theta_{CO} = 0.73 \pm 0.03$ has been obtained from several experiments of CO adsorption on clean Pt(111) (Fig. 2). Within experimental error, this value is the same as the one obtained from STM images (17).

A parameter which allows one to estimate the fraction of linear bonded CO in the total CO_{ads} population, n, has been used in this work, and is defined as the number of electrons involved in CO oxidation per platinum adsorption site liberated after CO oxidation,

$$n = \frac{Q_{CO}}{Q^{Bi}_{Pt} - Q^{CO}_{Pt}}, \quad [7]$$

where Q^{Bi}_{Pt} is the platinum adsorption charge after CO (Fig. 1B, dark shadowed area) oxidation and Q^{CO}_{Pt} (Fig. 5A, shadowed area) is the charge of the platinum adsorption sites after CO adsorption. An n value of 2 would mean that all CO molecules are in linear configuration. Lower n values indicates the presence of bridged-bonded or multibonded CO. This parameter is quite sensitive to the presence of nonlinear CO; small amounts of bridged-bonded CO significantly diminish the n values (24). For the experiment in Fig. 2, an n value of 1.50 is found.

An additional parameter has been used when the CO does not completely block the Bi + Pt(111) surface. S_b is defined as the fraction of hydrogen adsorption sites blocked by the CO:

$$S_b = 1 - \frac{Q^{CO}_{Pt}}{Q^{Bi}_{Pt}}. \quad [8]$$

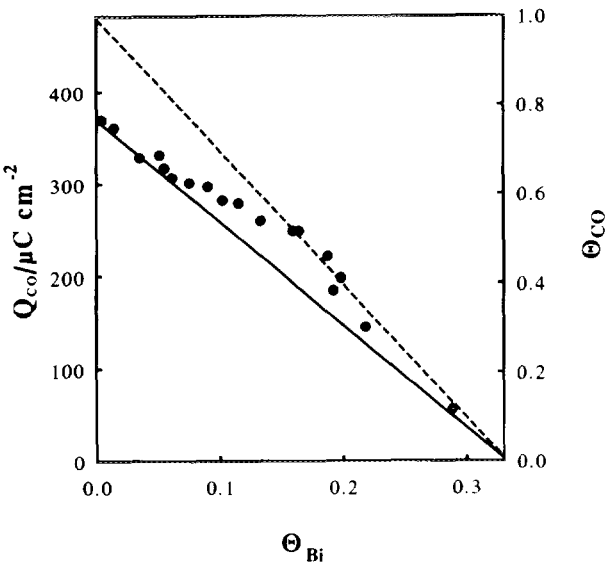

FIG. 7. Variation of the CO stripping charge (Q_{CO}) and Θ_{CO} with Θ_{Bi}.

In Fig. 7 the values of Q_{CO} (Θ_{CO}) for saturation CO coverages are plotted versus Θ_{Bi}. If the adsorbed CO maintained the same fraction of linearly bonded and bridged-bonded CO as on the clean Pt(111) electrode, a linear decrease would be expected. As at $\Theta_{Bi} = 0.33$ all the platinum adsorption sites have been blocked by bismuth, no CO adsorption occurs unless bismuth desorption takes place. For UHV systems, CO adsorption is completely inhibited at $\Theta_{Bi} = 0.38$ (7), similar to the results obtained in this work. The full line in Fig. 7 shows this ideal behavior. On clean Pt(111) surfaces, as the CO coverage diminishes, the fraction of linearly bonded CO also diminishes, yielding a less compact adlayer, i.e., lower n values (13, 14). Then, if bismuth behaved as a simple third body blocking three platinum atoms, without influence on the electronic properties of the surface, the diminution of CO coverage would lead to a less compact adlayer and to lower Θ_{CO} values than those represented by the full line for a given Θ_{Bi} (Fig. 7).

The behavior found is the opposite of that described above. Points deviate to higher CO coverages, indicating that bismuth does not act as a simple third body, but exerts some electronic influence on the properties of the surface. The increase in bismuth coverage leads to more compact adlayers. In Fig. 7, the dashed line represents the CO oxidation charge that would have been obtained if the CO were constituted only in linearly bonded CO. As can be seen, points at $\Theta_{Bi} > 0.15$ fit this latter line quite well.

The evolution of n values with the bismuth coverage (Fig. 8) is useful in studying the evolution of the fraction of linearly bonded CO. As already pointed out, on clean Pt(111) surfaces and at low bismuth coverages, the n value is approximately 1.50. This means that the linearly bonded CO is the predominant species, but there is still an important fraction of bridged-bonded CO, in good agreement with *in situ* FTIR experiments (13, 14). Parallel to the increase of bismuth coverage, there is an increase of n, reaching a contant value of 1.75 for $\Theta_{Bi} > 0.17$. To obtain such an n, 90% of the CO population should be in a linear form (24). For such a coverage Chang and Weaver (23) found that linear CO is almost the only species present on the surface.

The change in the fraction of linear CO indicates that bismuth has an electronic effect on the Bi + Pt(111) surfaces. This electronic effect has also been proposed in UHV because of the change in the fraction of linearly bonded CO with bismuth coverage (7). However, it is important to remark that there are different binding geometries for CO in electrochemical and UHV environments. In UHV the species predominant at low CO coverages is linearly bonded CO and the presence of bismuth leads to an increase in the bridged-bonded CO (7), whereas in electrochemical environments the behavior is the opposite (23).

An electronic effect has also been suggested for the inhibition of poison formation from formic acid on these surfaces (22). In this latter case, the presence of a small amount of bismuth at $\Theta_{Bi} = 0.04$ is able to inhibit poison formation completely (22). For CO adsorption, the electronic effect does not have so dramatic an influence, since at such low coverages the influence of the bismuth ada-

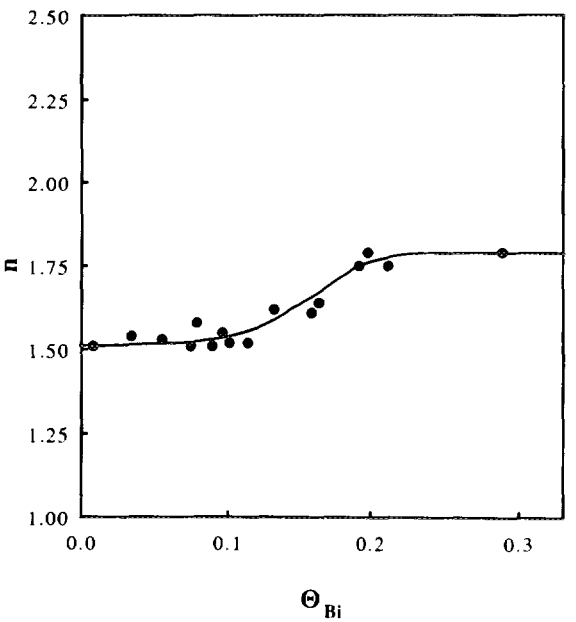

FIG. 8. Variation of n with Θ_{Bi}.

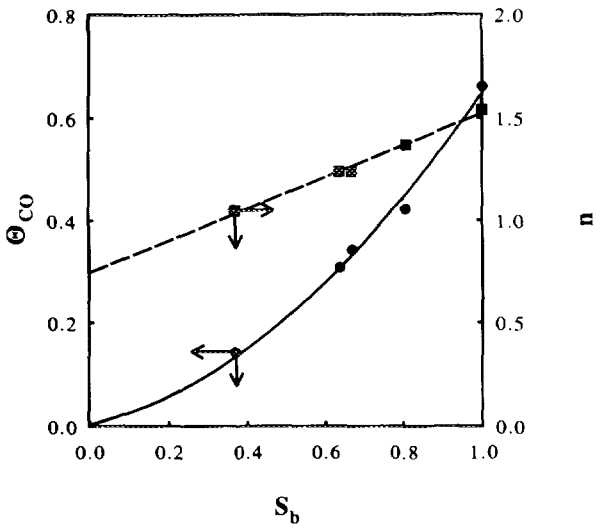

FIG. 9. Variation of Θ_{CO} and n with S_b for $\Theta_{Bi} = 0.05$.

toms is not perceptible, and it is only important at medium and high bismuth coverages.

It is also interesting to study the coverage and population distribution for nonsaturation CO coverages. Figure 9 shows the variation of Θ_{CO} and n with S_b at $\Theta_{Bi} = 0.05$. A linear relationship between Θ_{CO} and S_b is expected when CO always blocks the same number of platinum atoms. As discussed above, the deviation from linearity found in this case corresponds to the behavior expected for diminishing CO coverages on clean Pt(111). This is also reflected in the variation of n. For low S_b values, n is around 1, which indicates that the CO population is almost entirely constituted by nonlinear species. As the S_b increases, the value of n increases linearly until the value of 1.5 for CO saturation coverages is reached. This parallels the observations of the FTIR experiments for low bismuth coverages, where the fraction of linear CO diminishes as the CO coverage also diminishes (13, 14). It can be concluded that at this bismuth coverage the electronic influence of the adsorbed bismuth is not strong enough to produce important changes in the populations of CO with respect to the observations for unmodified Pt(111) electrodes.

Conversely, quite different behavior is observed at $\Theta_{Bi} = 0.15$ (Fig. 10). The Θ_{CO} variation with S_b is almost linear. It follows a straight line and n values are independent of the CO coverages, having the same value as that obtained for saturation coverages (1.65). This implies that the bismuth is having an influence on the surface properties, and the electronic effect has changed the population of the CO_{ads}. This influence seems to be independent of the Bi–CO lateral effects since at low CO coverages it cannot be detected.

Enhancement of Catalysis of CO Oxidation by Bismuth Adatoms

As pointed out above, the presence of bismuth adsorbed on the Pt(111) electrode has shifted the onset of CO stripping to more negative values with respect to the unmodified Pt(111) surface. This means that bismuth adsorbed on the Pt(111) surface enhances CO oxidation. To explain this catalytic effect two different mechanisms can be considered: (i) an electronic effect, and (ii) bifunctional catalysis. In the first case, bismuth would be assumed to modify the electronic properties of the surface in a way that promoted CO oxidation. In the latter, oxidized bismuth would transfer the oxygen group necessary for CO oxidation.

In the previous discussion, an electronic effect on CO populations has been found. This effect may be responsible for catalysis enhancement of the CO oxidation. Model calculations on platinum clusters with bismuth and CO indicate that bismuth donates 0.217 electrons to the platinum surface and this increases back-donation from platinum to the C–O bond (33). Therefore, a stabilization of the adsorbed CO molecule on platinum would be expected and CO oxidation on the bismuth-modified electrode would be retarded with respect to the unmodified electrode. Thus, the second possibility is the more probable, namely, that the observed catalysis takes place through bismuth-mediated oxygen transfer. The joint oxidation of CO and bismuth when CO is present on the surface indicates an intimate relationship between both oxidation processes. Moreover, if an electronic effect were responsible for the catalytic enhancement in CO oxidation, there would be no influence of the bismuth oxidation process on the CO oxidation.

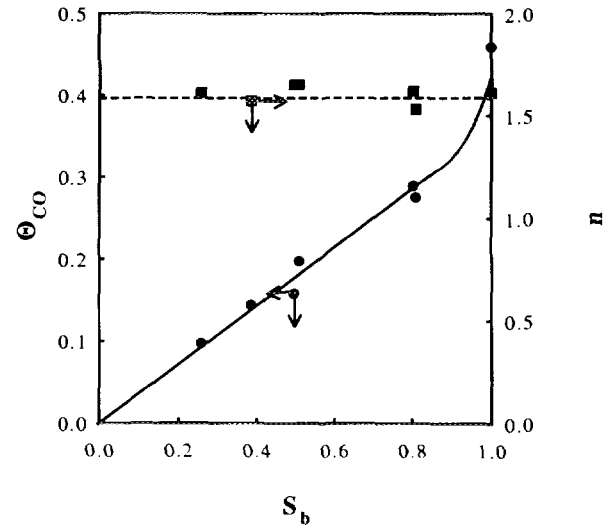

FIG. 10. Variation of Θ_{CO} and n with S_b for $\Theta_{Bi} = 0.15$.

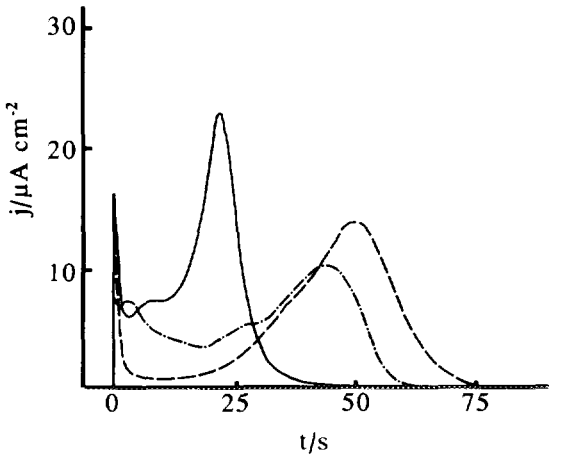

FIG. 11. Transient CO oxidation at 0.7 V for Pt(111) electrodes with $\Theta_{Bi} = 0.10$ and $\Theta_{CO} = 0.56$ (full line), $\Theta_{Bi} = 0.00$ and $\Theta_{CO} = 0.70$ (dashed-dotted line), and $\Theta_{Bi} = 0.00$ and $\Theta_{CO} = 0.54$ (dashed line).

It has been shown that after partial oxidation of the CO (Fig. 3), part of the bismuth redox peak has been recovered in the usual potential range. As has been pointed out, the oxidation form of the redox couple involves an oxygenated species ($Bi(OH)_2$ or BiO). These species can provide the oxygen necessary for the CO oxidation. This bismuth-mediated oxygen transfer can explain the voltammetric features described in Figs. 1A–1D. Saturation monolayers of CO retard the oxidation of surface bismuth. Once the oxidation of bismuth starts, oxygenated species of Bi(II) are generated and CO oxidation starts. Therefore, the surface bismuth oxidation process cannot be decoupled from CO oxidation since bismuth oxidation initiates CO oxidation.

To study this enhancement several current–time plots were recorded. In these experiments, after CO adsorption, the electrode was immersed at 0.1 V, a potential step at given potential was applied and the transient current recorded. Figure 11 shows the results obtained at CO saturation coverage ($\Theta_{CO} = 0.7$), for an intermediate CO coverage ($\Theta_{CO} = 0.54$) on unmodified Pt(111) electrodes, and for a CO saturation coverage ($\Theta_{CO} = 0.56$) on a Pt(111) electrode with $\Theta_{Bi} = 0.10$. This cannot be understood as an effect of the diminution of the CO coverage induced by the presence of bismuth, because CO oxidation is also faster than on the unmodified Pt(111) electrode with the same CO coverage. In fact, the correct comparison has to be done with saturation coverages, since the CO oxidation process occurs through a nucleation and growth process (34, 35). Therefore, the presence of free adsorption sites on the surface where water can absorb enhances the CO oxidation. For this reason, fully blocked surfaces have to be compared.

Despite the absence of free adsorption sites on the bismuth-covered electrode, the oxidation of CO occurs faster than on partially covered Pt(111) electrodes; therefore another source of oxygen, different from water, has been involved in the CO oxidation. This species has to be supplied by the bismuth adatoms on the surface. Catalysis enhancement similar to that depicted in Fig. 11 has been found for potentials higher than 0.65 V, where bismuth adatoms are oxidized. At lower potentials, no significant enhancement was detected, reinforcing the idea that the catalytic process is a bismuth-mediated oxygen transfer.

CONCLUSIONS

- Bi–CO adlayers present a microscopically mixed adlayer structure. This kind of structure has been proposed by studying the modification of the surface bismuth redox peak seen in the presence of CO.
- We report an accurate way of measuring CO coverages in the presence of bismuth adatoms from voltammetry. The CO coverages obtained agree with those in the literature (23).
- Bismuth adatoms influence the binding geometries of CO_{ads}. At medium Bi coverages almost the only species on the surface is linear CO, regardless of CO coverage. On unmodified Pt(111), it was found that there is an important contribution of bridged-bonded or multibonded CO species.
- The structure of the UHV Bi–CO adlayers (7) differs notably from that observed in electrochemical environments.
- Bismuth enhances the catalysis of CO oxidation by transferring oxygen to the CO molecules. The CO oxidation rate for a bismuth-covered electrode is faster than that found for an unmodified Pt(111) electrode at equivalent CO coverages.

ACKNOWLEDGMENTS

This work was partially supported by DGICYT Project CE 94-0031. One of us, E. H., acknowledges the Conselleria de Educació i Ciència of the Generalitat Valenciana for an FPI grant.

REFERENCES

1. Engel, T., and Ertl, G., *in* "Advances in Catalysis," Vol. 28 (D. D. Eley, H. Pines, and P. B. Weisz, Eds.), Academic Press, New York, 1979.
2. Goodman, D. W., *Acc. Chem. Res.* **17,** 194 (1984).
3. Malik, I. J., and Trenary, M., *Surf. Sci.* **214,** L237 (1989).
4. Wagner, F. T., Moylan, T. E., and Schmieg, S. J., *Surf. Sci.* **195,** 403 (1988).
5. Schwaizer, E., Persson, B. N. J., Tüshaus, M., Hoge, D., and Bradshaw, A. M., *Surf. Sci.* **213,** 49 (1989).
6. Persson, B. N. J., Tüshaus, M., and Bradshaw, A. M., *J. Chem. Phys.* **92,** 5034 (1990).
7. Paffett, M. T., Campbell, C. T., Windham, R. G., and Koel, B. E., *Surf. Sci.* **207,** 274 (1989).

8. Kiskinova, M. P., Szabó, A., and Yates, J. T., *Surf. Sci.* **226,** 237 (1990).
9. Clavilier, J., Faure, R., Guinet, G., and Durand, R., *J. Electroanal. Chem.* **107,** 205 (1980).
10. Clavilier, J., Feliu, J. M., and Aldaz, A., *J. Electroanal. Chem.* **243,** 419 (1988).
11. Beden, B., Bilmes, S., Lamy, C., and Leger, J. M., *J. Electroanal. Chem.* **149,** 295 (1983).
12. Furuya, N., Motoo, S., and Kunimatsu, K., *J. Electroanal. Chem.* **239,** 347 (1988).
13. Chang, S.-C., and Weaver, M. J., *J. Phys. Chem.* **92,** 4582 (1990).
14. Chang, S.-C., and Weaver, M. J., *Surf. Sci.* **238,** 142 (1990).
15. Kitamura, F., Takahashi, M., and Ito, M., *Surf. Sci.* **223,** 493 (1989).
16. Kinomoto, Y., Watanabe, S., Takahashi, M., and Ito, M., *Surf. Sci.* **242,** 538 (1991).
17. Villegas, I., and Weaver, M. J., *J. Chem. Phys.* **101,** 1648 (1994).
18. Feliu, J. M., Fernández-Vega, A., Orts, J. M., and Aldaz, A., *J. Chim. Phys.* **88,** 1493 (1991).
19. Evans, R. W., and Attard, G. A., *J. Electroanal. Chem.* **345,** 337 (1993).
20. Clavilier, J., Fernández-Vega, A., Feliu, J. M., and Aldaz, A., *J. Electroanal. Chem.* **258,** 89 (1988).
21. Campbell, S.-A., and Parsons, R., *J. Chem. Faraday Trans.* **88,** 833 (1992).
22. Herrero, E., Fernández-Vega, A., Feliu, J. M., and Aldaz, A., *J. Electroanal. Chem.* **350,** 73 (1993).
23. Chang, S.-C., and Weaver, M. J., *Surf. Sci.* **241,** 11 (1991).
24. Orts, J. M., Fernández-Vega, A., Feliu, J. M., Aldaz, A., and Clavilier, J., *J. Electroanal. Chem.* **327,** 261 (1992).
25. Clavilier, C., Rodes, A., El Achi, K., and Zamakhchari, M. A., *J. Chim. Phys.* **88,** 1291 (1989).
26. Clavilier, J., Armand, D., Sun, S. G., and Petit, M., *J. Electroanal. Chem.* **205,** 267 (1986).
27. Shibata, M., Takahasi, O., and Motoo, S., *J. Electroanal. Chem.* **249,** 253 (1988).
28. Feliu, J. M., Orts, J. M., Fernández-Vega, A., Aldaz, A., and Clavilier, J., *J. Electroanal. Chem.* **296,** 191 (1990).
29. Clavilier, J., Albalat, R., Gómez, R., Orts, J. M., Feliu, J. M., and Aldaz, A., *J. Electroanal. Chem.* **330,** 489 (1992).
30. Feliu, J. M., Orts, J. M., Gómez, R., Aldaz, A., Clavilier, J., *J. Electroanal. Chem.* **360,** 325 (1993).
31. Wieckowski, A., Zelenay, P., and Varga, K., *J. Chim. Phys.* **88,** 1247 (1991).
32. Faguy, P. W., Markovic, N., Adzic, R. R., Fierro, C. A., and Yeager, E. B., *J. Electroanal. Chem.* **289,** 245 (1990).
33. Lin, W.-F., Sun, S.-G., and Tian, Z.-W., *J. Electroanal. Chem.* **364,** 1 (1994).
34. McCallum, C., and Pletcher, D., *J. Electroanal. Chem.* **70,** 277 (1976).
35. Love, B., Lipkowski, J., *in* "ACS Symposium Series," Vol. 378 (M. P. Soriga, Ed.), Chap. 33. Washington, 1988.